
IPPRO: Importance-based Pruning with PProjective Offset for Magnitude-indifferent Structural Pruning

Jaeheun Jung*

Department of Mathematics
Korea University
Seoul, Republic of Korea
wodsos@korea.ac.kr

Jaehyuk Lee*

Department of Mathematics
Korea University
Seoul, Republic of Korea
jaehyeokbear@korea.ac.kr

Yeajin Lee,

Program in Actuarial Science
and Financial Engineering
Korea University
Seoul, Republic of Korea
gin1214@korea.ac.kr

Donghun Lee[†]

Department of Mathematics
Korea University
Seoul, Republic of Korea
holy@korea.ac.kr

Abstract

With the growth of demand on neural network compression methods, the structured pruning methods including importance-based approach are actively studied. The magnitude importance and many correlated modern importance criteria often limit the capacity of pruning decision, since the filters with larger magnitudes are not likely to be pruned if the smaller one didn't, even if it is redundant. In this paper, we propose a novel pruning strategy to challenge this dominating effect of magnitude and provide fair chance to each filter to be pruned, by placing it on projective space. After that, we observe the gradient descent movement whether the filters move toward the origin or not, to measure how the filter is likely to be pruned. This measurement is used to construct PROscore, a novel importance score for IPPRO, a novel importance-based structured pruning with magnitude-indifference. Our evaluation results shows that the proposed importance criteria using the projective space achieves near-lossless pruning by reducing the performance drop in pruning, with promising performance after the finetuning. Our work debunks the "size-matters" myth in pruning and expands the frontier of importance-based pruning both theoretically and empirically.

1 Introduction

Deep learning has achieved remarkable success in various application domains at the cost of ever-increasing computation and memory requirements. Overparametrization of neural networks is beneficial for convergence and generalization power of deep learning, but burdens resource-constrained platforms such as smartphones and edge devices. Motivated by this need for model compression, neural network pruning became a quintessential tool to curtail the computation and memory requirement of deep learning models [1]. In particular, structured pruning [2] emerged as a key pruning technique, as its explicit channel or filter-based pruning aligns well with modern computing architecture optimization and translates to significantly reduced memory footprint and FLOPs.

*equal contribution

[†]corresponding author

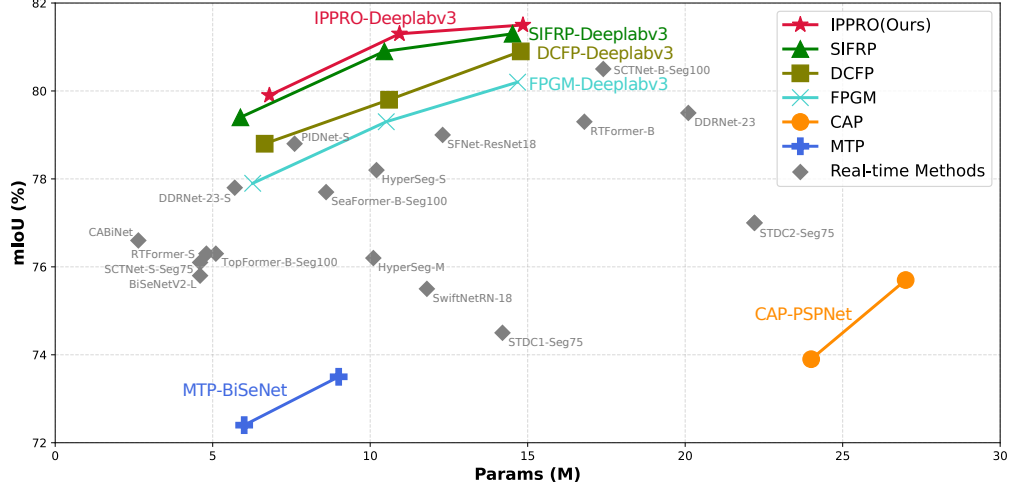


Figure 1: IPPRO (Importance-based Pruning with PProjective Offset) outperforms state-of-the-art pruning methods and expands the Pareto frontier on Cityscape dataset using Deeplabv3.

Regularization-based structured pruning uses regularizers such as Lasso [3, 4] or Group Lasso [5, 6] to decide filters to prune. Importance-based structured pruning ranks and prunes the filters with least importance scores. Although distinct, both approaches are closely related; regularization and importance measures often rely on each other for smarter pruning. For example, a common theme for both regularization-based and importance-based structural pruning is the magnitude of a filter, typically measured as the norm of each channel’s weight tensor [7].

Despite its intuitiveness, pruning based on filter magnitudes can be deceiving [8, 9]: imagine scaling a layer up and inversely scaling down the next layer – this procedure can arbitrarily perturb the filter magnitudes while preserving the model output. More refined structured pruning methods incorporate other criteria, such as gradient information via Taylor expansion [10] or geometric similarity of filter clusters [11]. However, even these efforts have not yet disentangled magnitude-norm based artifacts from their filter score metric of functional importance in structured pruning.

We address this limitation by proposing IPPRO, a novel magnitude-invariant importance-based structured pruning algorithm. Our key contribution is the construction of PROscore, a novel importance score with magnitude invariance established from projective geometry. To gain scale invariance, IPPRO maps filters to real projective space by augmenting each filter with its vector norm, and then computes PROscore from the filters’ dynamics under gradient flow, which completely decouples the filter weight vector from its magnitude.

IPPRO is conceptually simple, straightforward to implement, model architecture agnostic. As CNN-based vision models are the workhorses for on-device low-resource inference tasks, we validate IPPRO’s practical effectiveness on diverse vision benchmarks with its consistent performance even in high-pruning regimes and no fine-tuning scenarios. We formally define the theoretical foundations of PROscore in Section 3, describe implementation of IPPRO in Section 4, and present its comprehensive empirical evaluation in Section 5.

2 Related Works

2.1 Structured Pruning using Magnitudes

Deep Neural Networks (DNNs) are often overparameterized, leading to unnecessary computational costs. Pruning addresses this by removing unimportant weights or structures. Early methods like magnitude-based pruning [12] eliminate weights with small absolute values, achieving model compression with minimal accuracy loss. However, such approaches may overlook a weight’s actual impact on performance.

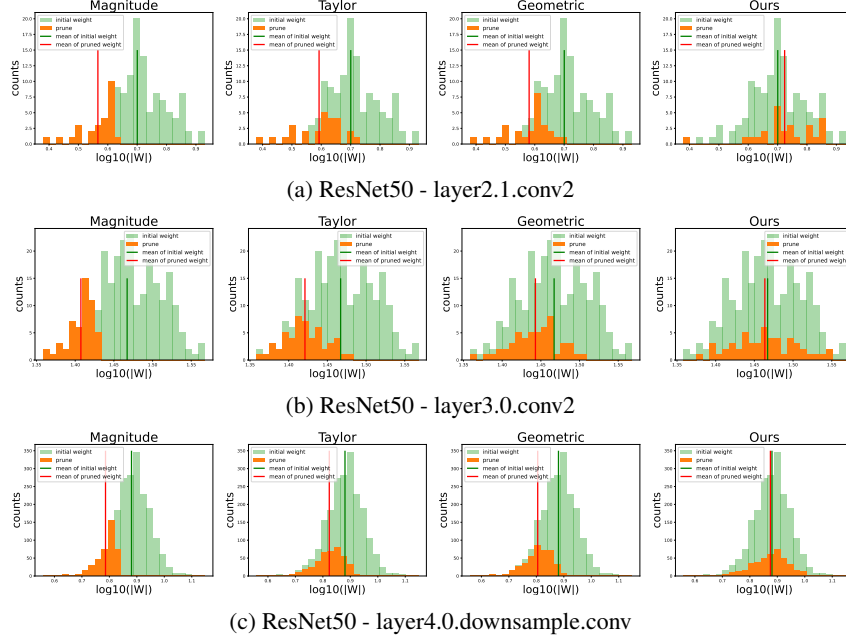


Figure 2: Visualization of magnitude of pruning filters obtained by four different criteria, on Resnet50 with ImageNet dataset.

To improve pruning effectiveness, gradient-based methods [13, 10] consider how changes in weights affect the loss function, enabling more informed decisions. Yet, determining optimal pruning ratios per layer is still challenging, as uniform pruning often leads to suboptimal results. Studies [7, 14] show that layers vary in pruning sensitivity, motivating adaptive approaches. Ye et al. [15] proposed the Sequential Greedy Pruning Strategy (SGPS), which iteratively removes weights based on layer-wise importance, achieving more balanced and performance-aware pruning.

2.2 Importance-based Pruning

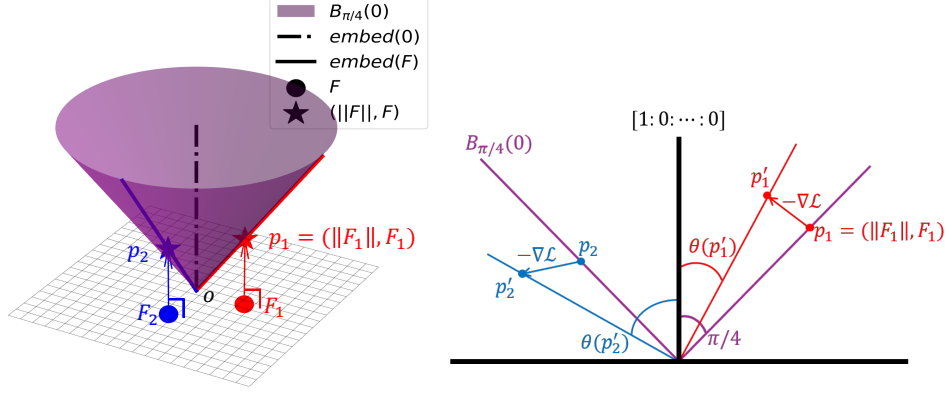
Importance-based pruning evaluates filter contribution to remove redundancy in CNNs. Norm-based methods like L_1 -norm [16] and L_2 -norm [17] prune low-magnitude filters, while others use filter similarity. For example, [11] uses the Geometric Median to remove closely clustered filters, and [18, 19] apply Scalar Hashing and Input-wise Splitting to detect and prune similar filters based on input relevance.

Statistical and structural approaches further enhance pruning. [20] uses Pearson Correlation to remove highly similar filters and applies Layer-wise Max-Normalization for cross-layer comparison. [21] treats filters as graph nodes to detect redundancy via structural properties. Recently, [22] introduced a torque-inspired method that weights filters by distance from a pivot, capturing spatial structure and offering a simple yet effective pruning strategy.

3 Methods

Let C be number of prunable channels in a neural network model, and $F_1, \dots, F_C \in \mathbb{R}^N$ be the filters which correspond to the channels. Each filter F_i is a vector, which has two distinct types of geometric information: magnitude and direction. We aim to design a novel pruning methodology that challenges the “size matters” myth in pruning, where ‘size’ is the magnitude of a prunable filter, as this myth limits the potential of magnitude-based pruning.

In Section 3.1, we introduce the concept of projective geometry, and define the mapping function *embed* which maps the filters to the projective space \mathbb{RP}^N . After placing the filters to \mathbb{RP}^N , in Section 3.2 we explain the distance in projective space given by an angular distance, and define the proposed importance using the angular distance.



(a) Visualization of $B_{\pi/4}(0)$ and $embed(F)$ in \mathbb{R}^{N+1} (b) Intuitive section plot for $\theta(p)$ explanation

Figure 3: Illustrations for conceptual understanding of PROScore for N -dimensional filter F .

3.1 Embedding Filters into Projective Space

To extract the directional information of a filter, which can complement its magnitude, we place the filter on a projective space with proper mapping $embed$, and specify the projective space which we utilized. In algebraic geometry, the (real) projective space \mathbb{RP}^N is defined as quotient of $\mathbb{R}^{N+1} - \{0\}$ under equivalence relation $x \sim cx$ for all positive real constant c , comprised of lines in \mathbb{R}^{N+1} passing through origin. The element of \mathbb{RP}^N can be expressed as $[v] = [v_0 : \dots : v_N]$ where

$$\forall c \neq 0, [v_0 : \dots : v_N] = [cv_0 : \dots : cv_N]. \quad (1)$$

The point $[v]$ of projective space \mathbb{RP}^N exactly corresponds to the line in \mathbb{R}^{N+1} whose direction vector is parallel to v and passing through 0.

Considering the filter as a vector in \mathbb{R}^N , we can find the embedding function which maps filter $F_i = (F_{i1}, \dots, F_{iN}) \neq 0$ to \mathbb{RP}^N by following function:

$$embed : (F_{i1}, \dots, F_{iN}) \mapsto [\|F_i\| : F_{i1} : \dots : F_{iN}]. \quad (2)$$

In Fig. 3a, we visualize how the filter F is mapped to the projective representation in $N = 2$ case. Note that $N = 2$ appears in practice when the target layer is batch normalization layer. For the zero filter 0_F , the embedding would be $[1 : 0 : \dots : 0]$, which corresponds to axis line of extra parameter in \mathbb{R}^{N+1} . Another benefit of this placement to \mathbb{RP}^N is that it naturally enjoys the magnitude-indifferent characteristic readily noticed by the scale invariance: $embed(cF) = embed(F)$ for $c > 0$.

3.2 PROScore: a Novel Pruning Importance Score

In projective space \mathbb{RP}^N , the distance between two points may be considered as an angle between two lines in \mathbb{R}^{N+1} where each line represents each point in \mathbb{RP}^N . If we denote $B_r(0)$ be the set of points in \mathbb{RP}^N whose angular distance between the origin is equal to r , then we can see that $Im(embed) \subseteq B_{\pi/4}(0)$; i.e. the distance between $embed(F)$ and the origin is always equal to $\pi/4$. This is visualized in Fig. 3a using line representations in \mathbb{R}^{N+1} that $B_{\pi/4}(0)$ becomes the cone centered at 0 and $embed(F)$ will become a line included in $B_{\pi/4}(0)$.

This phenomenon is exploited to ensure fair chance for the filters to be pruned, overcoming the sole dependency on the magnitude. After placing the filters to $B_{\pi/4}(0)$, we gauge the fate of each filters by estimating whether it would move closer to origin (and be pruned) or not, according to the direction of gradient descent. The direction for each filter F_i is represented by the angular distance $\theta(p'_i)$ between the origin and one-step forwarded point p'_i in \mathbb{RP}^N .

We define the tangent $\tan(\theta(p'_i))$ as a novel importance score for pruning decision of filter F_i , and name it **PROJECTIVE OFFSET SCORE (PROScore)**. Precisely, given $F_i = (F_{i1}, \dots, F_{iN})$ let D_i be extra variable initialized by $\|F_i\|$. Then the point $p_i = (\|F_i\|, F_i)$ would be updated to Eq. (3) by gradient

descent on loss function \mathcal{L} , and λ which is a hyperparameter that serves a similar role to weight decay in the loss function.

$$p'_i = \left(\|F_i\| - \lambda \frac{\partial \mathcal{L}}{\partial D_i}, F_i - \lambda \nabla_{F_i} \mathcal{L} \right) \quad (3)$$

And the PROscore is computed by

$$\tan(\theta(p'_i)) = \frac{\|F_i - \lambda \nabla_{F_i} \mathcal{L}\|}{\| \|F_i\| - \lambda \frac{\partial \mathcal{L}}{\partial D_i} \|}, \quad (4)$$

which would be the proposed importance score of i -th filter. As depicted in Fig. 3b, the i -th channel would have small $\theta(p_i)$ when the red-colored movement of gradient descent makes p_i closer and otherwise (the blue-colored arrow) not.

4 Implementation of IPPRO

We present **Importance-based Pruning with PProjective Offset (IPPRO)**, our implementation of structural pruning using PROscore presented in Section 3. First, we overview the parameter injection trick to realize the projective space embedding. Then, we present the algorithm to compute PROscore, our novel importance score for IPPRO, and conclude the section with the remaining implementation details.

4.1 Projective Offsetting via Parameter Injection

We implement the idea of embedding into the projective space as outlined in Section 3 by introducing additional parameter D with desired initialization $D^{init} = \text{diag}(\|F_1\|, \dots, \|F_N\|)$. To bring filters to projective space, we inject D parameter to the model using the extension method [23], which adds two identical parameters D and \overline{D} , by modifying element-wise computation layer σ , which appear next to the target layer W as follows:

$$\psi_{D, \overline{D}}(x) = Dx - \overline{D}x + \sigma(x). \quad (5)$$

The modification by $\psi_{D, \overline{D}}$ does not harm the model's functionality and performance, since D and \overline{D} are set to be same. The introduced parameters are removed to retrieve the original model before actual pruning happens, as they are needed for PROscore computation.

4.2 Computing PROscore

In Algorithm 1 we present the algorithm that we implemented to compute PROscore.

Algorithm 1: PROscore Computation

- 1: **Input** number of channels N , dataset \mathcal{D} , layer W , consecutive operation σ and model $f(W, \sigma)$
 - 2: Compute $D^{init} = \text{diag}(\|F_1\|, \dots, \|F_N\|)$
 - 3: Extend model to $f(W, \psi_{D, \overline{D}})$ using $\psi_{D, \overline{D}}$ in Eq. (5)
 - 4: Initialize $D, \overline{D} \leftarrow D^{init}$
 - 5: Compute $\nabla \mathcal{L}$ using backpropagation with \mathcal{D}
 - 6: Compute $\tan(\theta(p'_i))$ for all i 's by Eq. (4)
 - 7: **Return** the PROscore $\tan(\theta(p'_i))$ for each filter F_i
-

Given pretrained model with filters $F_i = W_{i,:}$, we compute D^{init} by line 2 of Algorithm 1, and extend the model by adding parameters to σ , which are initialized by D^{init} . The choice of σ would be followed by the choice of target layer. For example, if the target is scaling factor of batch normalization layer in ResNet then σ would be the ReLU activation. After extending model, we estimate the loss gradient using the training dataset via backpropagation. Finally, we compute the tangent value of angular distance $\theta(p'_i)$ between the origin and p'_i .

4.3 Implementation Overview

IPPRO computes the PROscore without updating model parameters. Gradients are accumulated across the full dataset, and pruning is applied to the original model using the precomputed scores.

Table 1: Comparison of pruning performance on ImageNet dataset

Model	Method	Top-1 Acc (%)			Top-5 Acc (%)			Params(↓%)	FLOPs(↓%)
		Base.	Prun.	Δ	Base.	Prun.	Δ		
ResNet-50	SFP [17]	76.15	74.61	-1.54	92.87	92.06	-0.81	N/A	2.3G(41.8)
	Autopruner [26]	76.15	74.76	-1.39	92.87	92.15	-0.72	N/A	2.1G(48.7)
	FPGM [11]	76.15	75.59	-0.56	92.87	92.63	-0.24	15G(37.5)	2.3G(42.2)
	Taylor [10]	76.18	74.50	-1.68	N/A	N/A	N/A	14G(44.5)	2.2G(44.9)
	GAL [27]	76.15	71.95	-4.20	92.87	90.94	-1.93	21G(16.9)	2.3G(43.0)
	HRank [28]	76.15	74.98	-1.17	92.87	92.33	-0.54	16G(36.6)	2.3G(43.7)
	SCOP [29]	76.15	75.95	-0.20	92.87	92.79	-0.08	14G(42.8)	2.2G(45.3)
	CHIP [25]	76.15	<u>76.15</u>	<u>0.00</u>	92.87	<u>92.91</u>	<u>+0.04</u>	14G(44.2)	2.1G(48.7)
	RGP[30]	76.22	75.30	-0.92	N/A	N/A	N/A	14G(43.8)	2.3G(43.8)
	FPBICI[31]	76.13	76.08	-0.05	92.86	92.85	-0.01	14G(45.9)	2.1G(50.4)
	IPPRO (ours)	76.15	76.21	+0.06	92.87	93.02	+0.15	13G(46.4)	2.1G(47.7)
	SCOP [29]	76.15	<u>75.26</u>	<u>-0.89</u>	92.87	92.53	-0.34	12G(51.8)	1.8G(54.6)
	SIRFP [32]	76.15	75.14	-1.01	92.87	93.12	+0.25	N/A	1.7G(58.7)
	CHIP [25]	76.15	<u>75.26</u>	<u>-0.89</u>	92.87	92.53	-0.34	11G(56.7)	1.5G(62.8)
	Torque [22]	76.07	74.58	-1.49	N/A	N/A	N/A	9G(64.5)	1.7G(57.2)
	FPBICI[31]	76.13	75.01	-1.12	92.86	92.30	-0.56	11G(57.7)	1.5G(63.8)
	IPPRO (ours)	76.15	75.51	-0.64	92.87	<u>92.67</u>	<u>-0.20</u>	10G(60.0)	1.6G(60.0)
	HRank [28]	76.15	69.10	-7.05	92.87	89.58	-3.29	8G(67.5)	0.9G(76.0)
	CHIP [25]	76.15	<u>73.30</u>	<u>-2.85</u>	92.87	<u>91.48</u>	<u>-1.39</u>	8G(68.6)	0.9G(76.7)
	RGP [30]	76.22	72.68	-3.54	N/A	N/A	N/A	6.4G(75.0)	1.0G (75.0)
	IPPRO (ours)	76.15	73.38	-2.77	92.87	91.50	-1.37	<u>6.5G(74.2)</u>	1.0G(74.2)
MobileNetV2	Meta [33]	74.70	<u>68.20</u>	<u>-6.50</u>	N/A	N/A	N/A	N/A	0.14G (54.2)
	GFP [34]	75.74	69.16	-6.58	N/A	N/A	N/A	N/A	0.15G (50.5)
	IPPRO (ours)	72.01	67.90	-4.11	90.62	88.04	-2.58	0.2G (42.3)	0.14G (54.2)

This design avoids iterative retraining during scoring and improves scalability. Further details of the implementation are provided in Appendix A.

To ensure fair comparisons, we follow standardized implementation protocols, including Torchvision-style preprocessing [24] and adopt [25] fine-tuning settings. We avoid augmentation tricks such as mixup to ensure reproducibility and controlled evaluation. Full details of the fine-tuning recipe and implementation specifications are provided in Appendix B.

5 Empirical Validations

We validate the effectiveness of IPPRO across diverse vision tasks, including image classification and semantic segmentation. Specifically, experiments are conducted on ResNet-50 and MobileNetV2 using ImageNet-1k, ResNet-56 on CIFAR-10, VGG19 on CIFAR-100, and DeepLabv3-ResNet50 on the Cityscapes dataset.

IPPRO is compared with state-of-the-art pruning methods such as Taylor [10], FPGM [11], Torque [22], SFP [17], and SCOP [29], as well as approaches leveraging non-magnitude cues like HRank [28], CHIP [25], and AutoPruner [26]. Across all benchmarks, IPPRO consistently delivers better or comparable performance with reduced model size.

We also examine sensitivity to fine-tuning and data sampling, confirming that IPPRO yields stable and favorable trade-offs between accuracy and model efficiency, effectively challenging the “size-matters” heuristics prevailing in neural network pruning methods.

5.1 Pruning Performance Analysis

We compare IPPRO with existing magnitude-based pruning methods, showing that it maintains or even improves baseline performance.

5.1.1 CIFAR-10 and CIFAR-100

We evaluated IPPRO on CIFAR-10 (ResNet-56) and CIFAR-100 (VGG19) using DepGraph pre-trained weights [35]. As shown in Table 2a, IPPRO reduces FLOPs and parameters by up to 49%

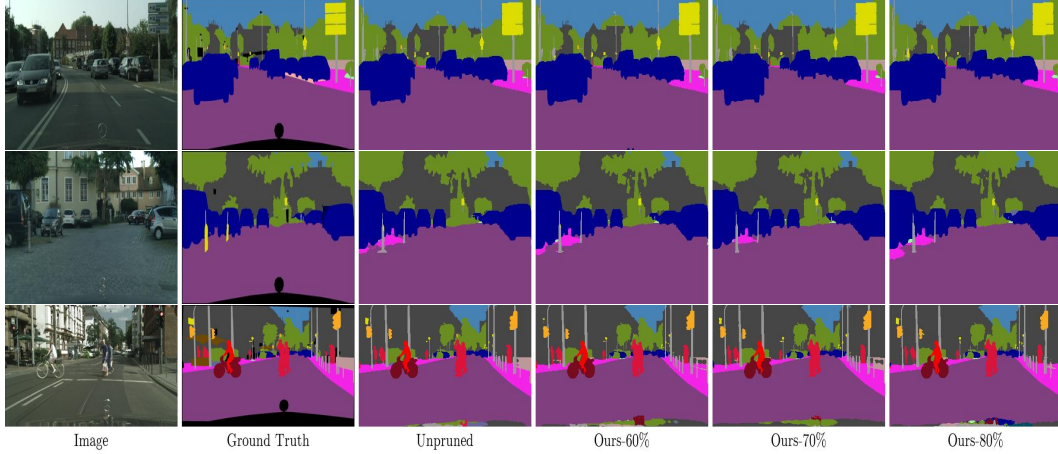


Figure 4: Qualitative segmentation results of IPPRO on the Cityscapes dataset using DeepLabv3.

on CIFAR-10 with a 0.55% accuracy gain. Even at higher compression rates (up to 77%), accuracy drops by only 1%, outperforming other methods. On CIFAR-100, IPPRO achieves 87% FLOPs and 87% parameter reduction with minimal accuracy loss, highlighting its effectiveness for compact, high-performing models.

5.1.2 ImageNet-1k

On ImageNet-1k, we evaluate IPPRO with ResNet-50 under three compression levels (47%, 60%, and 74% FLOPs reduction). As shown in Table 1, IPPRO improves Top-1 accuracy by 0.06% at moderate pruning and remains competitive at higher compression, outperforming state-of-the-art methods. Furthermore, for other FLOP reductions on 60% and 74%, IPPRO exhibited significantly higher accuracy compared to other superior methods.

We further validate IPPRO on MobileNetV2, a compact model without residual connections, where it shows the smallest accuracy drop at comparable FLOPs, demonstrating architectural versatility.

5.1.3 Segmentation

To further assess IPPRO, we apply it to a semantic segmentation task using DeepLabv3 with ResNet-50 on the Cityscapes dataset [46], following the experimental setup used by DCFP [43].

Table 2: Pruning Performance results of various tasks and datasets.

(a) CIFAR-10 and CIFAR-100							(b) Cityscapes - DeepLabV3-ResNet50						
Model Dataset	Method	Top-1 Acc (%)			Params (↓%)	FLOPs (↓%)	Method	mIoU			Params(↓%)	FLOPs(↓%)	
		Base.	Prun.	Δ				Base.	Prun.	Δ			
ResNet-56 CIFAR-10	Depgraph[35]	93.53	93.77	+0.24	-	-	Random	81.6	78.7	-2.9	59.8	60.6	
	HBFP[36]	93.26	92.42	-0.84	43.9	43.6	NS [3]	81.6	79.9	-1.7	62.3	59.4	
	GAL[27]	93.26	93.38	+0.12	12.3	37.6	Taylor[10]	81.6	80.3	-1.3	63.7	60.1	
	HRank[28]	93.26	93.52	+0.26	17.0	29.3	DepGraph[35]	81.6	80.0	-1.6	59.2	60.4	
	CHIP[25]	93.26	94.16	+0.90	43.9	47.4	FPGM[11]	81.6	80.2	-1.4	63.9	61.2	
	FPAC[37]	93.26	93.71	+0.45	42.8	47.4	DCFP[43]	81.6	80.9	-0.7	64.2	60.9	
	IPPRO (ours)	93.53	<u>94.06</u>	<u>+0.53</u>	49.7	49.3	FGP[44]	79.3	79.0	-0.3	64.4	60.4	
	HRank[28]	93.26	90.72	-2.54	68.4	74.1	SIRFP[45]	81.6	81.3	-0.3	64.8	61.3	
	HBFP[36]	93.26	91.79	-1.47	75.4	74.9	IPPRO (ours)	81.5	81.5	0.0	64.0	61.8	
	GAL[27]	93.26	91.58	-1.68	66.1	60.2	FPGM[11]	81.6	79.3	-2.3	74.5	71.0	
	CHIP[25]	93.26	<u>92.05</u>	<u>-1.21</u>	71.8	72.3	DCFP[43]	81.6	80.2	-1.4	74.3	71.3	
	SPSRC[38]	93.59	91.65	-1.94	64.7	63.9	SIRFP[45]	81.6	80.9	-0.7	74.4	71.9	
	IPPRO (ours)	93.53	92.47	-1.06	77.7	71.8	IPPRO (ours)	81.5	81.3	-0.2	73.5	70.9	
VGG19 CIFAR-100	Depgraph[35]	73.50	<u>70.39</u>	<u>-3.11</u>	-	88.7	FPGM[11]	81.6	77.9	-3.7	<u>84.8</u>	<u>80.7</u>	
	Kron-OBS[39]	73.34	60.66	-12.6	-	83.5	DCFP[43]	81.6	<u>79.5</u>	<u>-2.1</u>	83.9	80.2	
	Greg-2[40]	74.02	67.75	-6.27	-	88.6	SIRFP[45]	81.6	79.4	-2.2	85.7	81.6	
	EigenD[39]	73.34	65.18	-8.16	90.9	88.6	IPPRO (ours)	81.5	79.9	-1.6	83.0	80.1	
	Torque[41]	73.03	65.87	-7.16	90.8	88.7							
	GAT Transprunig[42]	73.26	66.68	-6.58	-	89.0							
	IPPRO (ours)	73.50	70.47	-3.03	87.9	87.5							

As seen in Table 2b, IPPRO maintains full mIoU performance at around 60% reduction of model size and consistently outperforms or matches other methods across various pruning levels. The qualitative segmentation results Fig. 4, along with additional examples in Fig. 6, do not show noticeable degradation. From left to right in Fig. 4: input image, ground truth, unpruned model, and IPPRO-pruned models with 60%, 70%, and 80% sparsity, respectively. These results confirm that IPPRO preserves high-level task performance, even at high pruning ratios, by maintaining semantic structure and object boundary quality.

5.1.4 Global Pruning

We define our importance score using angular deviation in the projective space, measuring how much each filter responds to data relative to a reference value of $\tan(\frac{\pi}{4})$. Although the absolute score can vary with the hyperparameter λ , PROscore enables global comparability without explicit normalization, unlike magnitude-based methods. This property is essential for global pruning, where importance scores must reside on a comparable scale to ensure fair competition among filters across layers. Without this, layers with intrinsically larger scores may be unjustly favored. To verify that score scaling induced by Eq. (4) λ does not undermine pruning behavior, we analyze its effect and confirm the stability of our method in Appendix G.

By leveraging this robust scoring scheme, our global pruning method consistently outperforms conventional magnitude-based global pruning. As shown in Table 3, it also achieves performance on par with other advanced approaches specifically designed to address the shortcomings of norm-based criteria.

5.2 Comparison of Importance Criteria

We compare IPPRO with other magnitude- and gradient-based pruning methods such as L_1 -norm [58], Taylor [10], and geometric [11]. For fairness, we compute gradients across the entire dataset, even for methods like Taylor that support randomized subsets. As shown in Table 4 and Fig. 2, traditional methods heavily depend on pre-trained weights and produce highly similar pruning patterns. In contrast, IPPRO demonstrates reduced reliance on initial weights, yielding distinct importance distributions. Histogram visualizations of ResNet-50 layers further confirm that IPPRO prunes differently, supporting its robustness against weight initialization bias.

5.3 Results without Finetuning

To examine whether the effectiveness of IPPRO depends heavily on fine-tuning, we evaluated its performance without any fine-tuning and compared it with L_1 -norm [58], Taylor [10], geometric [11], and random pruning methods. Using a uniform pruning ratio across all layers, IPPRO consistently outperformed all baselines on the ImageNet-1k dataset with ResNet-50, as shown in Fig. 5. On CIFAR-10, while most methods performed similarly at high FLOPs, IPPRO exhibited significantly less performance degradation as the pruning ratio increased, demonstrating its applicability in low-resource environments such as embedded or on-device setting. (Fig. 5).

Table 3: Global Pruning Performance results of ImageNet and CIFAR-10 datasets.

(a) ImageNet-1k on ResNet-50					(b) CIFAR-10 on ResNet-56				
Method	Top-1 Acc (%)			FLOPs(G)	Method	Top-1 Acc (%)			FLOPs(M)
	Base.	Prun.	Δ			Base.	Prun.	Δ	
ResConv-Prune[47]	76.2	70.0	-6.2	1.6	FSM[52]	93.26	93.63	+0.4	61.17
DBP-0.5[48]	76.2	72.4	-3.8	N/A	ITFCP[53]	93.39	93.60	+0.21	60.73
Meta[33]	76.2	73.4	-2.8	1.0	GCNNA[54]	93.72	93.72	0	58.29
AutoSlim[49]	76.2	74.0	-2.2	1.0	FSIM[55]	93.30	93.48	+0.18	59.24
GReg-2[40]	76.2	73.9	-2.3	1.3	IPPRO (ours)	93.53	94.00	+0.47	63.66
HALP[50]	76.2	74.5	-1.7	1.2	QSFm[56]	93.21	91.88	-1.33	50.62
IPPRO (ours)	76.2	74.6	-1.6	1.3	GBN[57]	93.10	91.76	-1.34	40.23
HALP[50]	76.2	68.1	-8.1	<u>0.6</u>	FSIM[55]	93.30	<u>91.96</u>	-1.34	31.08
MDP [51]	76.2	70.0	-6.2	0.5	IPPRO (ours)	93.53	92.43	-1.10	<u>37.49</u>
IPPRO (ours)	76.2	69.9	-6.3	<u>0.6</u>					

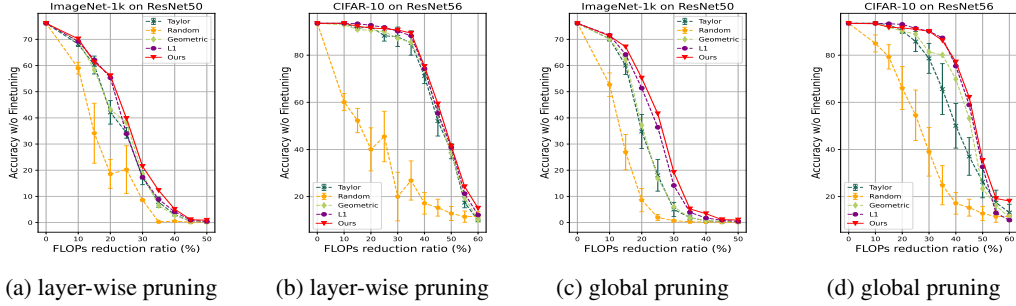


Figure 5: Without Finetuning Top-1 Accuracy results of different datasets

5.4 Sampling Sensitivity Analysis

To evaluate the robustness of our importance-score estimation, we tested the effect of using only a small subset (5–50%) of the training data when computing gradients. As summarized in Table 5, pruning performance remains nearly unchanged even with 5% of the data, while achieving significant computational speedups. For detailed analysis and experimental results, please refer to Appendix E.

6 Discussion

IPPRO outshines state-of-the-art methods in high-sparsity pruning regimes as demonstrated in Section 5.3. While conventional importance-based pruning methods are heavily influenced by filter magnitude, PROscore decouples pruning decision from filter magnitude and enables IPPRO to prune of both small and large-magnitude filters as necessary for effective pruning. In some cases, layer-wise pruning shows marginally better results (Table 1, Table 3a), yet IPPRO controls the risk of over-pruning often seen in global pruning schemes and maintains strong overall performance.

PROscore balances computational feasibility and informative scoring for importance-based pruning: computing full-batch gradient only once to estimate filter importance with high correlation to the eventual prune-or-preserve decision. Nevertheless, tracing the gradient descent trajectories beyond a single step may yield further refinement to stabilize and improve the importance score computation. Moreover, there may be a deeper connection between IPPRO and Catalyst [23], an emerging regularizer for lossless structural pruning motivated by the geometry of pruning-invariant model parameter subspace. This observation naturally leads to a research conjecture that PROscore-based pruning is related to Catalyst-based pruning and its empirical success is partially due to Catalyst’s theoretical guarantee of robust bifurcation between pruned and preserved filters.

Despite the demonstrated strengths, IPPRO has some limitations such as computational overhead facing large datasets as PROscore requires full-batch gradient. Our pilot research shown in Appendix E suggests that PROscore is surprisingly reliable even when only a subset of full-batch data is used, and this leads to natural future research direction of a stochastic counterpart of IPPRO for online structural pruning. Moreover, our empirical validations are confined to CNN-based models which represents most of current on-device vision models. Since PROscore is model-agnostic and IPPRO generally applicable to convolutional components such as ASPP in the DeepLabV3-ResNet50 model [59], further validation studies such as on Vision Transformers and Swin Transformers remain as valuable future work.

7 Conclusion

We introduce PROscore, a novel magnitude-invariant importance score for structural pruning. PROscore challenges conventional over-reliance on magnitude and takes a fundamentally different approach to gauge filter importance via angular displacement of filters under gradient descent in real projective space. We construct a novel pruning algorithm, IPPRO, as a theoretically well-founded innovation beyond the longstanding “size-matters” heuristics in structured pruning. Empirical validations on IPPRO shows superior performance in standard benchmark scenarios and robustness under extreme pruning conditions. By introducing and validating the novel theoretical perspective on

magnitude-decoupled importance-based pruning strategy, this work not only improves state-of-the-art performance but also offers a fresh lens of projective geometry for structural pruning research.

References

- [1] Lei Deng, Guoqi Li, Song Han, Luping Shi, and Yuan Xie. Model compression and hardware acceleration for neural networks: A comprehensive survey. *Proceedings of the IEEE*, 108(4):485–532, 2020.
- [2] Yang He and Lingao Xiao. Structured pruning for deep convolutional neural networks: A survey. *IEEE Transactions on Pattern Analysis and Machine Intelligence*, pages 1–20, 2023.
- [3] Zhuang Liu, Jianguo Li, Zhiqiang Shen, Gao Huang, Shoumeng Yan, and Changshui Zhang. Learning efficient convolutional networks through network slimming. In *Proceedings of the IEEE international conference on computer vision*, pages 2736–2744, 2017.
- [4] Hao Li, Asim Kadav, Igor Durdanovic, Hanan Samet, and Hans Peter Graf. Pruning filters for efficient convnets. In *International Conference on Learning Representations*, 2017.
- [5] Wei Wen, Chunpeng Wu, Yandan Wang, Yiran Chen, and Hai Li. Learning structured sparsity in deep neural networks. *Advances in neural information processing systems*, 29, 2016.
- [6] Baoyuan Liu, Min Wang, Hassan Foroosh, Marshall Tappen, and Marianna Pensky. Sparse convolutional neural networks. In *Proceedings of the IEEE conference on computer vision and pattern recognition*, pages 806–814, 2015.
- [7] Jian-Hao Luo, Jianxin Wu, and Weiyao Lin. Thinet: A filter level pruning method for deep neural network compression. In *Proceedings of the IEEE international conference on computer vision*, pages 5058–5066, 2017.
- [8] Yang He, Ping Liu, Ziwei Wang, Zhilan Hu, and Yi Yang. Filter pruning via geometric median for deep convolutional neural networks acceleration. In *Proceedings of the IEEE/CVF Conference on Computer Vision and Pattern Recognition (CVPR)*, June 2019.
- [9] Zhuang Liu, Mingjie Sun, Tinghui Zhou, Gao Huang, and Trevor Darrell. Rethinking the value of network pruning. In *International Conference on Learning Representations*, 2018.
- [10] Pavlo Molchanov, Arun Mallya, Stephen Tyree, Iuri Frosio, and Jan Kautz. Importance estimation for neural network pruning. In *Proceedings of the IEEE/CVF conference on computer vision and pattern recognition*, pages 11264–11272, 2019.
- [11] Yang He, Ping Liu, Ziwei Wang, Zhilan Hu, and Yi Yang. Filter pruning via geometric median for deep convolutional neural networks acceleration. In *Proceedings of the IEEE/CVF conference on computer vision and pattern recognition*, pages 4340–4349, 2019.
- [12] Song Han, Huizi Mao, and William J Dally. Deep compression: Compressing deep neural networks with pruning, trained quantization and huffman coding. *arXiv preprint arXiv:1510.00149*, 2015.
- [13] Davis Blalock, Jose Javier Gonzalez Ortiz, Jonathan Frankle, and John Guttag. What is the state of neural network pruning? *Proceedings of machine learning and systems*, 2:129–146, 2020.
- [14] Zhuang Liu, Jianguo Li, Zhiqiang Shen, Gao Huang, Shoumeng Yan, and Changshui Zhang. Learning efficient convolutional networks through network slimming. In *Proceedings of the IEEE international conference on computer vision*, pages 2736–2744, 2017.
- [15] Hancheng Ye, Bo Zhang, Tao Chen, Jiayuan Fan, and Bin Wang. Performance-aware approximation of global channel pruning for multitask cnns. *IEEE Transactions on Pattern Analysis and Machine Intelligence*, 45(8):10267–10284, 2023.
- [16] Hao Li, Asim Kadav, Igor Durdanovic, Hanan Samet, and Hans Peter Graf. Pruning filters for efficient convnets. In *International Conference on Learning Representations*, 2017.

- [17] Yang He, Guoliang Kang, Xuanyi Dong, Yanwei Fu, and Yi Yang. Soft filter pruning for accelerating deep convolutional neural networks. *arXiv preprint arXiv:1808.06866*, 2018.
- [18] Edouard Yvinec, Arnaud Dapogny, Matthieu Cord, and Kevin Bailly. Red: Looking for redundancies for data-free structured compression of deep neural networks. *Advances in Neural Information Processing Systems*, 34:20863–20873, 2021.
- [19] Edouard Yvinec, Arnaud Dapogny, Matthieu Cord, and Kevin Bailly. Red++: Data-free pruning of deep neural networks via input splitting and output merging. *IEEE Transactions on Pattern Analysis and Machine Intelligence*, 45(3):3664–3676, 2022.
- [20] Wenxiao Wang, Cong Fu, Jishun Guo, Deng Cai, and Xiaofei He. Cop: Customized deep model compression via regularized correlation-based filter-level pruning. *arXiv preprint arXiv:1906.10337*, 2019.
- [21] Zi Wang, Chengcheng Li, and Xiangyang Wang. Convolutional neural network pruning with structural redundancy reduction. In *Proceedings of the IEEE/CVF conference on computer vision and pattern recognition*, pages 14913–14922, 2021.
- [22] Arshita Gupta, Tien Bau, Joonsoo Kim, Zhe Zhu, Sumit Jha, and Hrishikesh Garud. Torque based structured pruning for deep neural network. In *2024 IEEE/CVF Winter Conference on Applications of Computer Vision (WACV)*, pages 2699–2708, 2024.
- [23] Anonymous. Catalyst pruning: Lossless structured pruning via algebraically principled regularization. Under Review, 2025.
- [24] TorchVision maintainers and contributors. Torchvision: Pytorch’s computer vision library. <https://github.com/pytorch/vision>, 2016.
- [25] Yang Sui, Miao Yin, Yi Xie, Huy Phan, Saman Aliari Zonouz, and Bo Yuan. Chip: Channel independence-based pruning for compact neural networks. *Advances in Neural Information Processing Systems*, 34:24604–24616, 2021.
- [26] Jian-Hao Luo and Jianxin Wu. Autopruner: An end-to-end trainable filter pruning method for efficient deep model inference. *Pattern Recognition*, 107:107461, 2020.
- [27] Shaohui Lin, Rongrong Ji, Chenqian Yan, Baochang Zhang, Liujuan Cao, Qixiang Ye, Feiyue Huang, and David Doermann. Towards optimal structured cnn pruning via generative adversarial learning. In *Proceedings of the IEEE/CVF conference on computer vision and pattern recognition*, pages 2790–2799, 2019.
- [28] Mingbao Lin, Rongrong Ji, Yan Wang, Yichen Zhang, Baochang Zhang, Yonghong Tian, and Ling Shao. Hrank: Filter pruning using high-rank feature map. In *Proceedings of the IEEE/CVF conference on computer vision and pattern recognition*, pages 1529–1538, 2020.
- [29] Yehui Tang, Yunhe Wang, Yixing Xu, Dacheng Tao, Chunjing Xu, Chao Xu, and Chang Xu. Scop: Scientific control for reliable neural network pruning. *Advances in Neural Information Processing Systems*, 33:10936–10947, 2020.
- [30] Zhuangzhi Chen, Jingyang Xiang, Yao Lu, Qi Xuan, Zhen Wang, Guanrong Chen, and Xiaoni Yang. Rgp: Neural network pruning through regular graph with edges swapping. *IEEE Transactions on Neural Networks and Learning Systems*, 2023.
- [31] Xiaolong Tang, Shuo Ye, Yufeng Shi, Tianheng Hu, Qinmu Peng, and Xinge You. Filter pruning based on information capacity and independence. *IEEE Transactions on Neural Networks and Learning Systems*, 2024.
- [32] Dongyue Wu, Zilin Guo, Li Yu, Nong Sang, and Changxin Gao. Structural pruning via spatial-aware information redundancy for semantic segmentation. *arXiv preprint arXiv:2412.12672*, 2024.
- [33] Zechun Liu, Haoyuan Mu, Xiangyu Zhang, Zichao Guo, Xin Yang, Kwang-Ting Cheng, and Jian Sun. Metapruning: Meta learning for automatic neural network channel pruning. In *Proceedings of the IEEE/CVF international conference on computer vision*, pages 3296–3305, 2019.

- [34] Liyang Liu, Shilong Zhang, Zhanghui Kuang, Aojun Zhou, Jing-Hao Xue, Xinjiang Wang, Yimin Chen, Wenming Yang, Qingmin Liao, and Wayne Zhang. Group fisher pruning for practical network compression. In *International Conference on Machine Learning*, pages 7021–7032. PMLR, 2021.
- [35] Gongfan Fang, Xinyin Ma, Mingli Song, Michael Bi Mi, and Xinchao Wang. Depgraph: Towards any structural pruning. In *Proceedings of the IEEE/CVF Conference on Computer Vision and Pattern Recognition*, pages 16091–16101, 2023.
- [36] SH Shabbeer Basha, Mohammad Farazuddin, Viswanath Pulabaigari, Shiv Ram Dubey, and Snehasis Mukherjee. Deep model compression based on the training history. *Neurocomputing*, 573:127257, 2024.
- [37] Huoxiang Yang, Yongsheng Liang, Wei Liu, and Fanyang Meng. Filter pruning via attention consistency on feature maps. *Applied Sciences*, 13(3):1964, 2023.
- [38] Xinglong Sun and Humphrey Shi. Towards better structured pruning saliency by reorganizing convolution. In *Proceedings of the IEEE/CVF Winter Conference on Applications of Computer Vision*, pages 2204–2214, 2024.
- [39] Chaoqi Wang, Roger Grosse, Sanja Fidler, and Guodong Zhang. Eigendamage: Structured pruning in the kronecker-factored eigenbasis. In *International conference on machine learning*, pages 6566–6575. PMLR, 2019.
- [40] Huan Wang, Can Qin, Yulun Zhang, and Yun Fu. Neural pruning via growing regularization. *arXiv preprint arXiv:2012.09243*, 2020.
- [41] Arshita Gupta, Tien Bau, Joonsoo Kim, Zhe Zhu, Sumit Jha, and Hrishikesh Garud. Torque based structured pruning for deep neural network. In *Proceedings of the IEEE/CVF Winter Conference on Applications of Computer Vision*, pages 2711–2720, 2024.
- [42] Yu-Chen Lin, Chia-Hung Wang, and Yu-Cheng Lin. Gat transpruning: progressive channel pruning strategy combining graph attention network and transformer. *PeerJ Computer Science*, 10:e2012, 2024.
- [43] Zixiao Wang, Hongtao Xie, Yuxin Wang, Hai Xu, and Guoqing Jin. Dcfp: Distribution calibrated filter pruning for lightweight and accurate long-tail semantic segmentation. *IEEE Transactions on Circuits and Systems for Video Technology*, 34(7):6063–6076, 2023.
- [44] Qingsong Lv, Jiasheng Sun, Sheng Zhou, Xu Zhang, Liangcheng Li, Yun Gao, Sun Qiao, Jie Song, and Jiajun Bu. Fgp: Feature-gradient-prune for efficient convolutional layer pruning. *arXiv preprint arXiv:2411.12781*, 2024.
- [45] Dongyue Wu, Zilin Guo, Li Yu, Nong Sang, and Changxin Gao. Structural pruning via spatial-aware information redundancy for semantic segmentation. In *Proceedings of the AAAI Conference on Artificial Intelligence*, volume 39, pages 8368–8376, 2025.
- [46] Marius Cordts, Mohamed Omran, Sebastian Ramos, Timo Rehfeld, Markus Enzweiler, Rodrigo Benenson, Uwe Franke, Stefan Roth, and Bernt Schiele. The cityscapes dataset for semantic urban scene understanding. In *Proceedings of the IEEE conference on computer vision and pattern recognition*, pages 3213–3223, 2016.
- [47] Pengtao Xu, Jian Cao, Fanhua Shang, Wenyu Sun, and Pu Li. Layer pruning via fusible residual convolutional block for deep neural networks. *arXiv preprint arXiv:2011.14356*, 2020.
- [48] Wenxiao Wang, Shuai Zhao, Minghao Chen, Jinming Hu, Deng Cai, and Haifeng Liu. Dbp: Discrimination based block-level pruning for deep model acceleration. *arXiv preprint arXiv:1912.10178*, 2019.
- [49] Jiahui Yu and Thomas Huang. Autoslim: Towards one-shot architecture search for channel numbers. *arXiv preprint arXiv:1903.11728*, 2019.
- [50] Maying Shen, Hongxu Yin, Pavlo Molchanov, Lei Mao, Jianna Liu, and Jose M Alvarez. Structural pruning via latency-saliency knapsack. *Advances in Neural Information Processing Systems*, 35:12894–12908, 2022.

- [51] Xinglong Sun, Barath Lakshmanan, Maying Shen, Shiyi Lan, Jingde Chen, and Jose Alvarez. Multi-dimensional pruning: Joint channel, layer and block pruning with latency constraint. *arXiv preprint arXiv:2406.12079*, 2024.
- [52] Yuanzhi Duan, Yue Zhou, Peng He, Qiang Liu, Shukai Duan, and Xiaofang Hu. Network pruning via feature shift minimization. In *Proceedings of the Asian conference on computer vision*, pages 4044–4060, 2022.
- [53] Yihao Chen and Zefang Wang. An effective information theoretic framework for channel pruning. *arXiv preprint arXiv:2408.16772*, 2024.
- [54] Di Jiang, Yuan Cao, and Qiang Yang. On the channel pruning using graph convolution network for convolutional neural network acceleration. In *IJCAI*, pages 3107–3113, 2022.
- [55] Yajun Liu, Kefeng Fan, Dakui Wu, and Wenju Zhou. Filter pruning by quantifying feature similarity and entropy of feature maps. *Neurocomputing*, 544:126297, 2023.
- [56] Zidu Wang, Xuexin Liu, Long Huang, Yunqing Chen, Yufei Zhang, Zhikang Lin, and Rui Wang. Qsfm: Model pruning based on quantified similarity between feature maps for ai on edge. *IEEE Internet of Things Journal*, 9(23):24506–24515, 2022.
- [57] Zhonghui You, Kun Yan, Jinmian Ye, Meng Ma, and Ping Wang. Gate decorator: Global filter pruning method for accelerating deep convolutional neural networks. *Advances in neural information processing systems*, 32, 2019.
- [58] Yihui He, Xiangyu Zhang, and Jian Sun. Channel pruning for accelerating very deep neural networks. In *Proceedings of the IEEE international conference on computer vision*, pages 1389–1397, 2017.
- [59] Liang-Chieh Chen, George Papandreou, Iasonas Kokkinos, Kevin Murphy, and Alan L Yuille. Deeplab: Semantic image segmentation with deep convolutional nets, atrous convolution, and fully connected crfs. *IEEE transactions on pattern analysis and machine intelligence*, 40(4):834–848, 2017.

A Implementation Detail

Note that the model parameters are not updated during the PROscore computation. The extended model is reverted to the original model and then we prune the filters according to the obtained PROscore.

To reduce the randomness of the empirical results of our implementation, we fixed the pre-trained weights W and the parameter D obtained from the extended projective space computed using the pre-trained weights. Also, we accumulate the gradients $\nabla_{F_i} \mathcal{L}$ and $\frac{\partial \mathcal{L}}{\partial D_i}$ from each batch of the backpropagation process using the entire dataset \mathcal{D} , unless otherwise mentioned.

Using the accumulated gradient values, along with the original model weights and the expanded parameter D , the layer-wise PROscore is computed according to Eq. (4). Using the PROscore, layer-wise pruning is performed on the original base model, which does not include the extended parameter D using the previously computed importance scores.

B Finetune Recipe

In this section, we detail the hyper-parameters used for fine-tuning. All or some of the models were fine-tuned using the PyTorch 1.13 framework on a Nvidia RTX 4090 GPU. Additionally, we emphasize that we did not use external data augmentation skills such as Color-jitter or Mix-up, which often employed to improve the performance in other pruning methods, since it invokes ethical issue on fair-comparison, as pretrained model did not used them and results with additional augmentation may not show the advantage of pruning method only.

B.1 ImageNet-1k dataset

For Importance score estimation on the ImageNet-1k dataset, we accumulated gradients over all data for one epoch for both ResNet-50 and MobileNetV2. For ResNet-50, fine-tuning was performed for a total of 180 epochs with a batch size of 128, using the SGD optimizer and a StepLR scheduler with a step size of 40. The initial learning rate was set to 0.01, with weight decay of 10^{-4} and momentum of 0.9, while the norm weight decay was $5e-5$ and the momentum was 0. For MobileNetV2, fine-tuning was carried out for 300 epochs with a batch size of 256, using the SGD optimizer and a cosine scheduler. The initial learning rate was also set to 0.01, with weight decay of 10^{-4} and momentum of 0.9.

B.2 CIFAR-10 dataset

On the CIFAR-10 dataset, for the ResNet-56 model with 71.8% FLOPs reduction, fine-tuning was conducted for 400 epochs with a batch size of 256, using the SGD optimizer and a cosine scheduler with a step size of 30. The initial learning rate was 0.025, with weight decay and momentum set to 0.0005 and 0.9, respectively. The same configuration was applied to the data size experiments for ResNet-56 in Table 5. For the ResNet-56 model with 49.3% FLOPs reduction, the same fine-tuning settings were used: 400 epochs, batch size of 256, SGD optimizer, cosine scheduler, initial learning rate of 0.03, and weight decay and momentum of 0.0005 and 0.9, respectively.

B.3 CIFAR-100 dataset

On the CIFAR-100 dataset, for the VGG-19 model with 87.5% FLOPs reduction, fine-tuning was conducted for 400 epochs with a batch size of 256, using the SGD optimizer and a cosine scheduler. The initial learning rate was 0.017 with weight decay and momentum set to 0.005 and 0.9, respectively.

C Pruning ratios

We provide the detailed layer-wise pruning ratios used for all models in our experiments. For each architecture, pruning rates are adjusted per layer group to account for differences in pruning sensitivity and to preserve overall performance.

- ResNet-50 (47.7%) : 0.25 for Downsample layer and 0.4 for the rest.

- ResNet-50 (60%) : 0.35 for Downsample layer and 0.45 for the rest.
- ResNet-50 (74.2%) : 0.45 for Downsample layer and 0.6 for the rest.
- MobileNetV2 (54.2%) : 0.2 for the first layer and 0.35 for the rest
- ResNet-56 (49.3%) : 0.15 for Downsample layer and 0.4 for the rest.
- ResNet-56 (71.8%) : 0.3 for Downsample layer, 0.6, 0.65 and 0.7 for the 1st, 2nd and 3rd blocks respectively.
- VGG19 (87.5%) : 0.65 for first 8 blocks, 0.7 for the next 4 blocks, and 0.6 for the rest.

D Importance score Correlation Table

Table 4 presents the pairwise correlation of importance scores among four pruning methods—Magnitude (L1-norm), Taylor, Geometric, and our proposed method—on ResNet-50 trained on ImageNet-1k.

The results reveal that traditional methods exhibit high similarity, indicating a shared reliance on pre-trained weight distributions. In contrast, our method shows lower correlation with them, suggesting it captures a distinct notion of importance.

Table 4: Correlation of ResNet-50 on Imagenet-1k between different magnitude based pruning methods.

Method	Magnitude	Taylor	Geometric	IPPRO
Magnitude	1.000	0.682	0.809	0.033
Taylor	0.682	1.000	0.433	0.064
Geometric	0.809	0.433	1.000	0.003
IPPRO (ours)	0.033	0.064	0.003	1.000

E Sensitivity Analysis

IPPRO computes importance scores by accumulating gradients, as defined in Eq. (4), resulting in linear time complexity with respect to the number of input samples. While using the full dataset ensures maximum accuracy, it incurs substantial computational cost. To evaluate the trade-off between efficiency and performance, we analyze the sensitivity of gradient-based importance estimation to the number of samples used.

We conduct experiments on ResNet-56 with CIFAR-10 and VGG-19 with CIFAR-100, varying the number of samples used to 100%, 50%, 25%, and 5% of the dataset. A balanced label sampler is employed to preserve label distribution across mini-batches. To account for randomness introduced by subset sampling, each configuration is repeated five times, and both the mean (Mu) and the maximum accuracy are reported.

As shown in Table 5, our method exhibits minimal accuracy degradation even when using as little as 5% of the dataset for importance score computation. This indicates that IPPRO is robust to subset-based sampling during pruning. Moreover, this implies immense empirical speedup potential of our implementation without sacrificing pruning performance.

Table 5: Experimental results on different dataset size

(a) CIFAR10 dataset on Resnet-56 (FLOPs reduction 71.85%)

Dataset size	Time usage (s)	Top-1 Acc (%)		
		Base.	Prun. Mu (Max)	Δ Mu (Max)
Full	45.4	93.53	92.47	-1.06
50%	25.4	93.53	92.18 (92.44)	-1.35 (-1.09)
25%	16.6	93.53	92.27 (92.46)	-1.26 (-1.07)
5%	7.2	93.53	92.21 (92.43)	-1.32 (-1.10)

(b) CIFAR100 dataset on VGG19 (FLOPs reduction 87.5%)

Dataset size	Time usage (s)	Top-1 Acc (%)		
		Base.	Prun. Mu (Max)	Δ Mu (Max)
Full	13.2	73.5	70.47	-3.03
50%	6.9	73.5	69.66(70.09)	-3.84(-3.41)
25%	3.5	73.5	69.55(70.03)	-3.95(-3.47)
5%	0.7	73.5	69.58(70.24)	-3.92(-3.26)

F Qualitative Results of DeeplabV3

In this section, we present qualitative results of the segmentation task. We compare the original image, ground truth segmentation, segmentation result from the unpruned model, and the segmentation result after pruning using our PROscore.

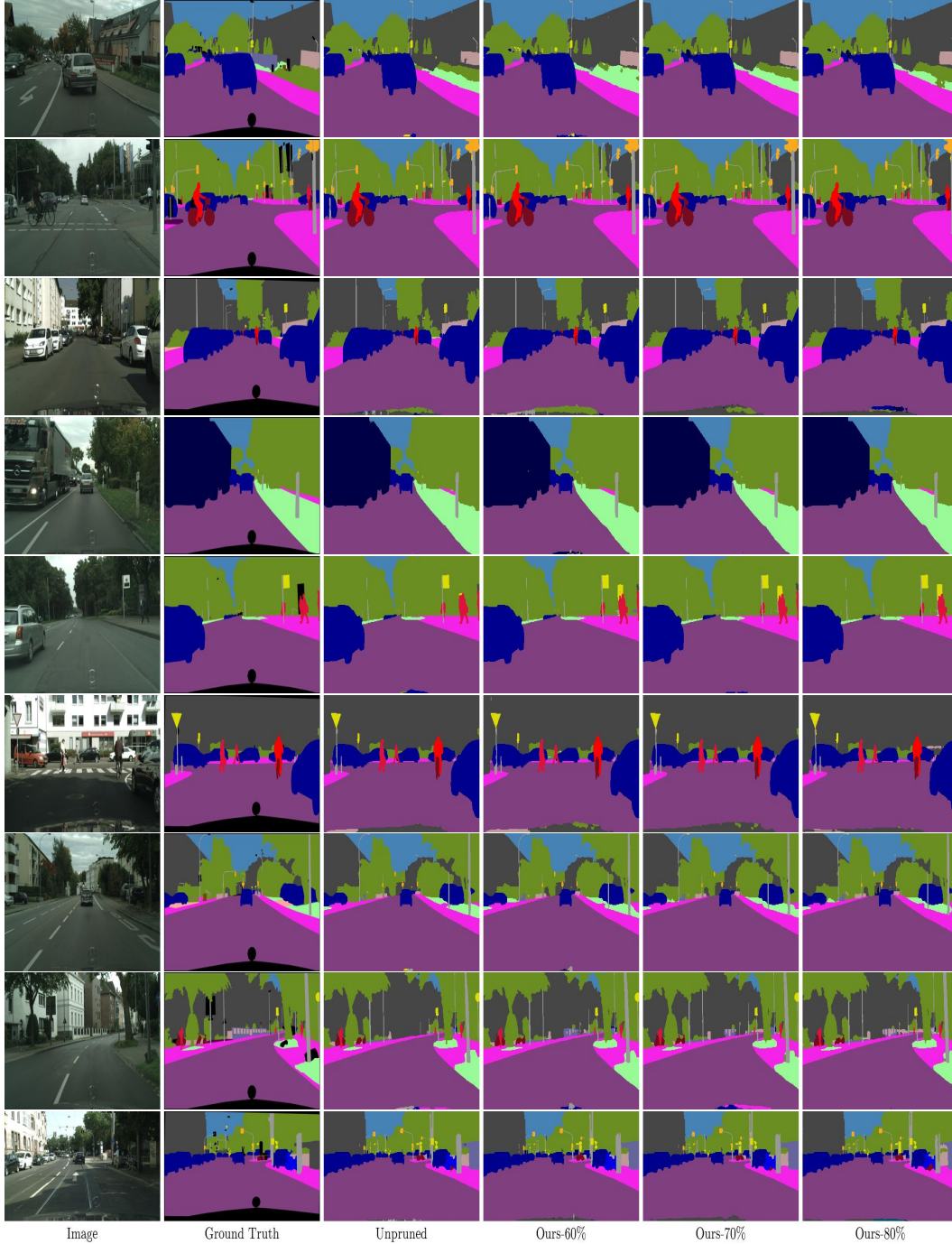


Figure 6: Visualization CitySpace dataset Our Pruning results of using DeeplabV3-ResNet50 models

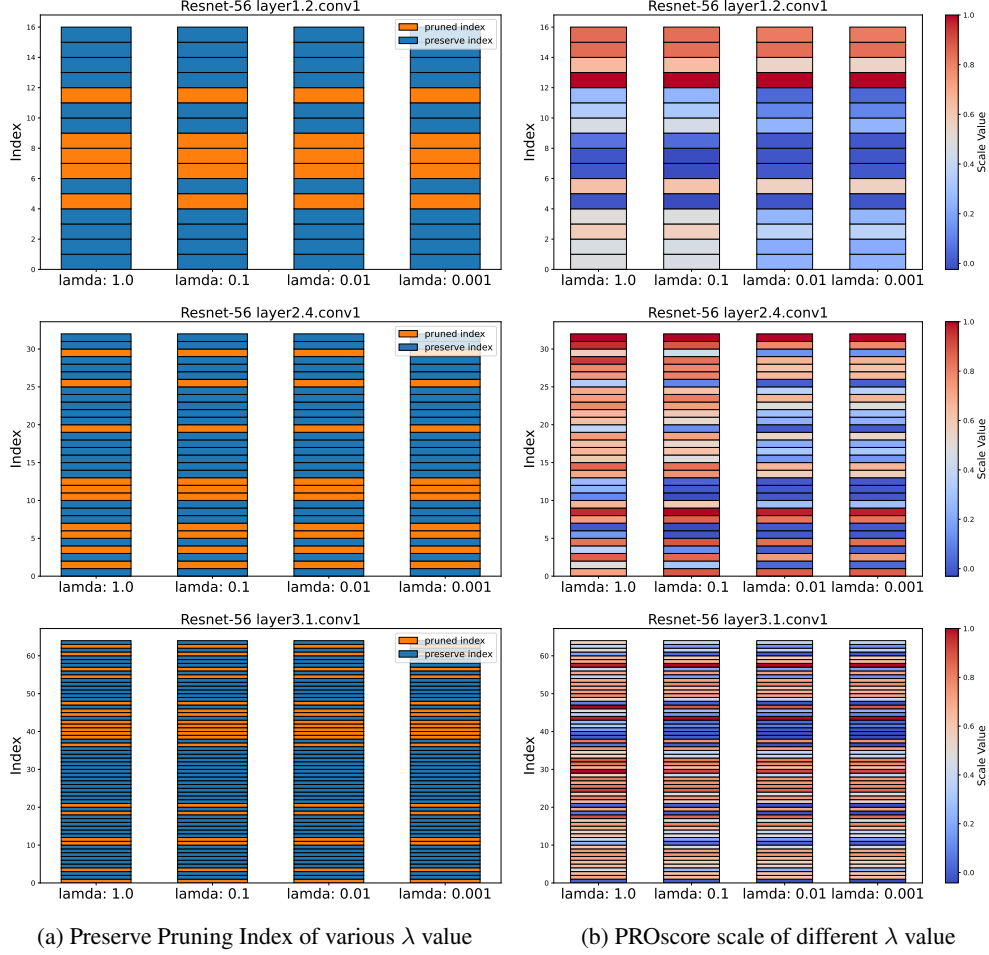


Figure 7: Preserve pruning index of λ changes

G Sensitivity Analysis of λ value

The absolute value of PROscore is affected by the hyperparameter λ , which controls the step size of the gradient movement in real projective space \mathbb{RP}^N , since the angle $\theta(p'_i)$ is related to the length $\overline{p_i p'_i}$. In extreme case, if $\lambda \rightarrow 0$ then $\theta(p'_i) \rightarrow \frac{\pi}{4}$ and thus the PROscores would distribute close to one.

However, the pruning decision are invariant under selection of isotropic scaling on $\lambda > 0$, since we are choosing filters with respect to their relative order which are invariant: if the p''_i is new point under gradient movement with different step size λ , then following holds: if $\theta(p'_i) < \theta(p'_j)$ then $\theta(p''_i) < \theta(p''_j)$.

To validate this, we conduct experiments on Resnet56 model with λ set to 1, 0.1, 0.01, and 0.001, examining both the preservation of pruning indices and the consistency of PROscore scales across layers. As shown in Fig. 7a, the pruning indices remained stable regardless of the λ value, and Fig. 7b shows that the relative importance measured by PROscore is invariant under λ selection.